The Motion Suspension System – MSS: A Cable-Driven System for On-Ground Tests of Space Robots

Ferdinand Elhardt[1,2(✉)], Roland Boumann[2], Marco De Stefano[1], Robin Heidel[2], Patrik Lemmen[2], Martin Heumos[1], Christoph Jeziorek[2], Maximo A. Roa[1], Manfred Schedl[1], and Tobias Bruckmann[2]

[1] Institute of Robotics and Mechatronics, DLR, Oberpfaffenhofen, Germany
ferdinand.elhardt@dlr.de

[2] Chair of Mechatronics, University of Duisburg-Essen, Duisburg, Germany

Abstract. Robotic manipulators play an important role in space exploration and pave the way for satellite lifetime extensions, orbital asset inspections, and deorbiting. However, space robots are tested in Earth's gravity although they are designed for zero gravity. The joints are limited in the torque which might be below of what is necessary to move on ground. To address this challenge, the paper presents the Motion Suspension System (MSS), a novel suspension system for on-ground tests of space robots which allows functional tests in the full, three-dimensional workspace. It is based on a cable-driven parallel robot controlled in admittance mode. The mechanical interface and the optimal gravity compensation strategy are optimized for maximum joint torque reduction. The cables are actuated using direct-drive motors. For demonstrating the feasibility of the MSS, we provide experimental results using the compliant CAESAR (CAESAR: Compliant Assistance and Exploration SpAce Robot) space robot arm by the German Aerospace Center (DLR).

Keywords: Space robotics · Cable-driven parallel robot · Gravity compensation · Offload mechanism · Suspension system · On-ground tests

1 Introduction

Robotic manipulators play a crucial role in space exploration. Free-flying robots mounted on satellites or space stations pave the way for manifold possibilities in future space mission: servicing, repairing and lifetime-extensions for commercial satellites, and removing of space debris. Since 2001, the 17 m *Canadarm2*[1] on the International Space Station assists with docking maneuvers, assembly, and maintenance in space. One of the key challenges with a space robot is the fact

[1] www.asc-csa.gc.ca/eng/iss/canadarm2.

M. Okada (Ed.): IFToMM WC 2023, MMS 148, pp. 379–388, 2023.
https://doi.org/10.1007/978-3-031-45770-8_38

that once it is deployed, it cannot be easily modified or repaired. This makes realistic on-ground testing of the robotic system a core need of the development to ensure reliability and to verify the robot performance.

Apart from environmental qualification targeting vacuum, radiation and temperature, the electro-mechanical assembly and the application software need to undergo rigorous tests [5]. This includes vision algorithms, teleoperation and autonomous controllers for providing the space robot with meaningful skills. However, since space robots are designed for operating in space, on-ground tests are challenging. Some space robots are non-gravity-bearing and thus too weak to move on Earth's gravity environment as they are designed to bear only zero-gravity loads [16].

On-ground validation of non-gravity-bearing space robots poses several challenges. Usually, advanced facilities are required to test space robots under 1g conditions while simulating floating base dynamics. Most space robot test facilities are based on planar/rotational air bearings, neutral buoyancy, free-fall/parabolic flights, helium balloons, or mechanical suspension systems [8,16]. Neutral buoyancy can be archived by underwater facilities [4] but hydrodynamics effects distort the motion [10]. The timespan of parabolic flights is too short for developing and testing robotic systems [21] and helium balloons introduce drag and high inertia. When using air bearings, the space robot is mounted on several pads which are movable on a horizontal flat surface. Pressured gas flowing through the bearing leads to a thin layer of gas between the floor and the pads. This enables the pads to move nearly friction-less in a horizontal plane [15,22]. However, Yao et al [24] describe the altering of the space robot's dynamics due to air bearings which forms a significant disadvantage – apart from the limitation to planar movements and the impact of the floor's inevitable unevenness. Mechanical suspension systems promise to tackle these drawbacks. Many of them use a Gantry crane for horizontal positioning. The vertical force can be applied passively using counterweights [3,7] or actively using motors [9] with both concepts introducing strong influence on the robot's dynamics due to high inertia. Thus, all traditional space robot test facilities suffer from different drawbacks hampering the on-ground qualification of space robots.

To reduce these disadvantages, we present a novel approach of suspending a non-gravity-bearing space robot: The cable-driven Motion Suspension System (MSS). The MSS, illustrated in Fig. 1, reduces the torque loads on a non-gravity-bearing space robot such that it can move in Earth's gravity. It also allows to use a larger, three-dimensional workspace of the space robot. Cable-driven parallel robots are used e.g. in automated construction [12,14,23], logistics [17,18], or rehab purposes [11]. The cables are connected to a mobile platform with multiple degrees of freedom and wound on motorized cable drums. Pulleys deflect the cables into the workspace. The MSS profits from the cable-based parallel robot's advantages, namely lightweight design, large workspace and high dynamics [25]. This makes it particular suitable for gravitational offloading.

This study introduces the MSS hardware design and the coupling interface required to connect the robot, followed by preliminary experimental results. Our

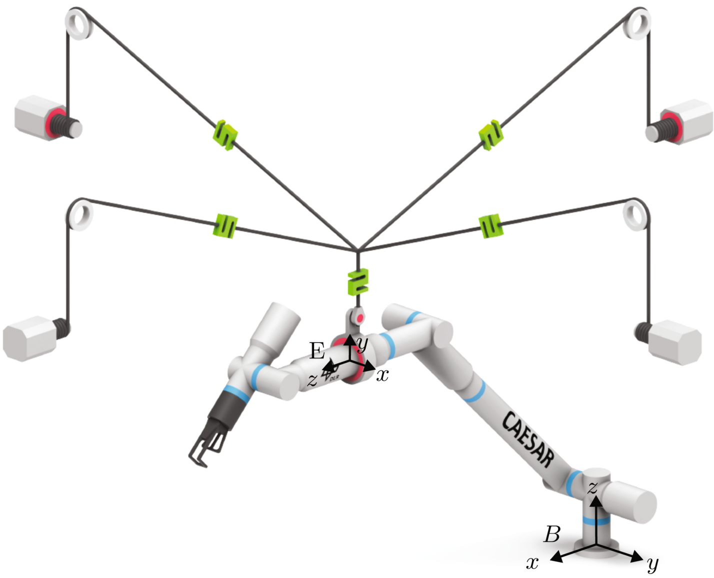

Fig. 1. The MSS suspends a robot arm and enables it to move in a large, three-dimensional workspace. The cable force sensors are illustrated in green.

approach paves the way for new possibilities not only in qualification of the space robot arm mechanics, but also in testing and qualifying high-level applications such as autonomous grasping and vision-based servoing.

The structure of this paper is the following: Sect. 2 introduces the coupling interface design of the MSS. Section 3 describes the robot on a functional level and provides component details. Section 4 illustrates preliminary experimental results of the MSS and Sect. 5 concludes the paper.

2 Coupling Interface Design

The MSS and the space robot are two independent systems which are connected at coupling frame E as shown in Fig. 1. The MSS applies forces in three Cartesian directions which are represented as the *suspension force* ${}_B\boldsymbol{f}_C \in \mathbb{R}^3$ w.r.t the fixed-base coordinate frame B. Note that no torques can be applied by the MSS on the space robot. Following the notation by De Stefano et al [6], the position of the coupling frame E determines the set of the influenceable space robot joints $A = \{x | x \in \mathbb{N}, x \leq i\}$ which consists of the joints from base joint 1 until the joint before the coupling interface i. Set N contains the non-influenceable joints from coupling interface to the space robot's tool center point. These joints cannot be supported by the MSS and thus need to be gravity-bearing for themselves.

To reconstruct the acting *suspension force* ${}_B\boldsymbol{f}_C$, the MSS uses the available position sensor data and a kinematic model of the space robot. See Table 1 for sensor details. As shown in Fig. 2, the coupling interface features an axial joint

($\alpha \in \mathbb{R}$) and a tangential joint ($\theta \in \mathbb{R}$), both passive and orthogonal. They result in the rotation matrices ${}_E\boldsymbol{A}_{E'}(\alpha) \in \mathbb{R}^{3x3}$ and ${}_{E'}\boldsymbol{A}_C(\theta) \in \mathbb{R}^{3x3}$. A force sensor provides the *suspension force* magnitude $f \in \mathbb{R}$, composed of ${}_C\boldsymbol{f}_C(f) = \begin{bmatrix} 0 & f & 0 \end{bmatrix}^\mathsf{T}$ w.r.t the *suspension force* frame C. The kinematic information of the space robot is described as a rotation matrix ${}_B\boldsymbol{A}_E \in \mathbb{R}^{3x3}$ from fixed base frame B to coupling frame E. Based on this, the suspension force is reconstructed by

$$ {}_B\boldsymbol{f}_C = \underbrace{{}_B\boldsymbol{A}_E\,{}_E\boldsymbol{A}_{E'}(\alpha)\,{}_{E'}\boldsymbol{A}_C(\theta)}_{{}_B\boldsymbol{A}_C(\alpha,\theta)}\;{}_C\boldsymbol{f}_C(f), \tag{1} $$

where ${}_B\boldsymbol{A}_C(\alpha, \theta) \in \mathbb{R}^{3x3}$ forms the total rotation matrix from fixed base frame B to *suspension force* frame C.

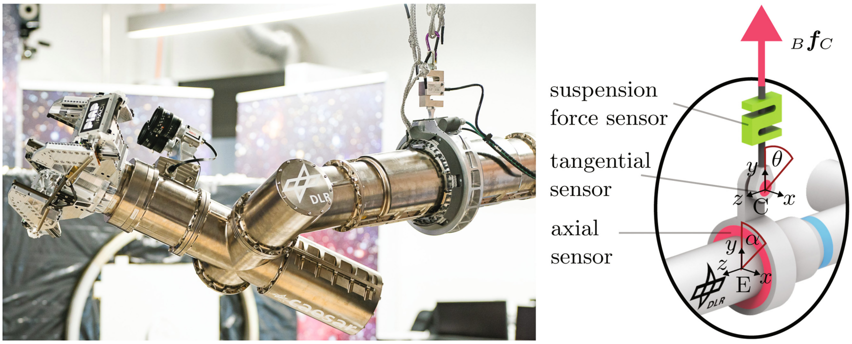

Fig. 2. The MSS coupling interface with the DLR space robot CAESAR (left). The coupling interface (right) connects the MSS with the robot manipulator.

The strategy to compute the desired *suspension force* ${}_B\boldsymbol{f}_{C,\text{des}}$ is based on the knowledge of the dynamics and configuration of the space robot. This leads to the required gravity torques $\boldsymbol{g}_A$ for the influenceable joints in set A. Based on this, the strategy provides internal joint torques $\boldsymbol{\tau}_{gA}$ for the space robot and the external desired *suspension force* ${}_B\boldsymbol{f}_{C,\text{des}}$ for the MSS. Details are presented in De Stefano et al [6] and the approach is based on the minimization problem

$$ \min_{(\boldsymbol{\tau}_{gA},\ {}_B\boldsymbol{f}_C)} \quad \frac{1}{2}\begin{bmatrix}\boldsymbol{\tau}_{gA}^T & {}_B\boldsymbol{f}_C{}^T\end{bmatrix}\begin{bmatrix}\boldsymbol{W}_{\boldsymbol{\tau}} & \boldsymbol{0} \\ \boldsymbol{0} & \boldsymbol{W}_{\boldsymbol{f}}\end{bmatrix}\begin{bmatrix}\boldsymbol{\tau}_{gA} \\ {}_B\boldsymbol{f}_C\end{bmatrix} \tag{2} $$

$$ \text{s.t. } \boldsymbol{g}_A = \boldsymbol{\tau}_{gA} + \boldsymbol{J}_{cA}^T\ {}_B\boldsymbol{f}_C \tag{3} $$

where $\boldsymbol{W}_{\boldsymbol{\tau}} \in \mathbb{R}^{i\times i}$ and $\boldsymbol{W}_{\boldsymbol{f}} \in \mathbb{R}^{3\times 3}$ are the weighting matrices for the joint torques and external wrench components and $\boldsymbol{J}_{cA}$ is the Jacobian at the coupling frame E. The output will satisfy the equality constraint for achieving full gravity compensation on the space robot. The gravity compensation torque for the joints in set N is computed directly from the space robot dynamics model, see [6] for details.

3 The MSS Design

A detailed analysis was performed for a specific robot arm, CAESAR, with an arm length of 3 m. This arm length requires from the suspension system a spherical cap working envelop with 2.2 m radius and 2.5 m height. This is represented by the green, spherical area shown in Fig. 3, where the MSS will be able to apply between 100 N to 750 N *suspension force* magnitude in z. The *Wrench-Feasible Workspace* which meets all requirements is shown in blue and was calculated by determining feasible cable force distributions on a discrete grid using the Closed-Form-Method described by Pott et al [19]. The forces in the four cables are denoted with $\tilde{\boldsymbol{f}} \in \mathbb{R}^4$. In order to follow the space robot's movements, a speed of $1.5\,\mathrm{m\,s^{-1}}$ and acceleration of $0.75\ \mathrm{m\ s^{-2}}$ w.r.t. the fixed base frame B is required. The sensors available on the MSS are shown in Table 1, with corresponding resolution and accuracy. The sensors on the cables and interface are visualized in Figs. 1 and 2, respectively.

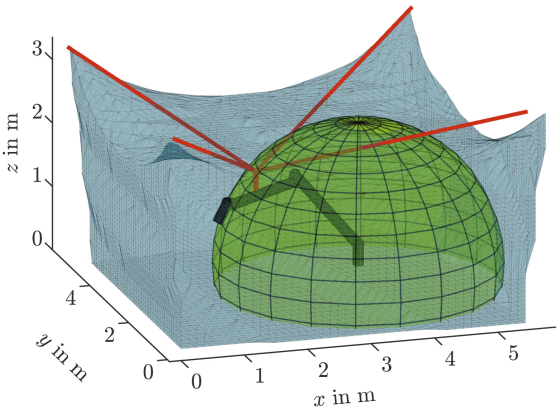

Fig. 3. The Wrench-Feasible Workspace (blue) of the MSS and the workspace required by the space robot (green) with the minimum cable forces $\tilde{f}_{\min} = 5\,\mathrm{N}$ and maximum cable force $\tilde{f}_{\max} = 1000\,\mathrm{N}$ for the desired *suspension force* z magnitude ${}_{B}f_{C,z} = 100\ \mathrm{N}$ to 750 N.

The drivetrain of the MSS consists of four PD-controlled direct drive servo motors featuring 80 N m rated torque. This leads to 1600 N rated cable forces limited to the maximum cable force $\tilde{f}_{\max} = 1000\,\mathrm{N}$ for safety reasons by software. To avoid slack cables, a minimum cable force $\tilde{f}_{\min}$ is required. The cables, 6 mm Dyneema with a tensile strength of 50 kN, transfer the forces from the winches via pivoting pulleys to the suspension force frame C of the space robot. The cable forces are measured by force sensors (details see Table 1).

Table 1. Sensors details as used in the MSS

Sensor	Range	Resolution	Accuracy
Axial interface rotation	Multiturn	26 bit	1.46″
Tangential interface rotation	Multiturn	22 bit	0.01°
Suspension force sensor	0 N to 1000 N	24 bit	0.02 %
Cable force sensors	0 N to 2000 N	24 bit	0.1 %
Winch motor encoders	Multiturn	24 bit	Unknown

3.1 Cable Robot Control

The MSS features a cascaded control circuit shown in Fig. 4. The inner loop for trajectory $\boldsymbol{x}_{\text{des}}$ control consists of an augmented PD controller [13] in joint space (which is defined using the cable lengths). As feedback, it uses the motor encoder measurements $\boldsymbol{\varphi}$ (see Table 1 for details) as well as cable and winch models. Using the MSS's Jacobian, the controller's output is the dynamic wrench $\boldsymbol{w}_{\text{dyn}}$ applied at the cable connection above frame C (shown in Fig. 2). The dynamic wrench is decomposed into desired cable forces $\tilde{\boldsymbol{f}}_{\text{des}}$ using a cable force calculation active-set algorithm [18]. The MSS drive units take the desired cable forces as input.

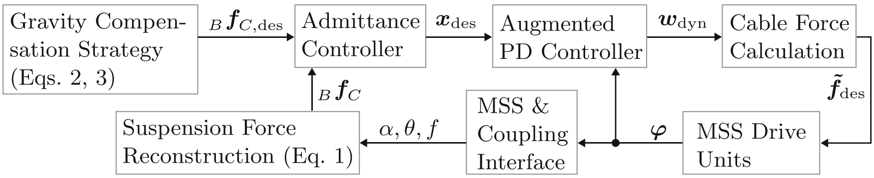

Fig. 4. The cascaded MSS control structure regulating the suspension force.

In the outer loop, an admittance variant controller [20] is used to track the *suspension force* ${}_B\boldsymbol{f}_{C,\text{des}}$. The main idea is altering the MSS trajectory in $\boldsymbol{x}_{\text{des}}$ in order to generate the desired *suspension force* which is requested by the gravity compensation strategy (Eqs. 2, 3). The admittance controller acts as a virtual spring-mass-damper system, reacting to the suspension force error with a dynamic displacement of $\boldsymbol{x}_{\text{des}}$.

The cable robot controller is computed in real time at 2 kHz using a compiled *Matlab Simulink* module. The state machine runs at 4 kHz using *Beckhoff TwinCAT3* on an industrial PC. The *EtherCAT* protocol is used as fieldbus and for communication with the space robot [1]. Fault detection, isolation, and recovery concepts are implemented in certified *Safety over EtherCAT* in order to ensure functional safety.

4 Experimental Validation and Discussion

As a preliminary experiment, we suspend the space robot DLR CAESAR (Compliant Assistance and Exploration SpAce Robot) [2] with the MSS. The CAESAR robot has 7 degrees of freedom, is designed for operating in space and cannot support its own weight on ground. In our experiment, the MSS is mounted such that the set of influenceable joints[2] is $A = \{1, 2, 3, 4\}$. CAESAR performs a trajectory which is shown in Fig. 5 using a joint position controller. It starts in a stretched-out position (a) close to the resting table, elevates (b) and ends in a contracted configuration (c).

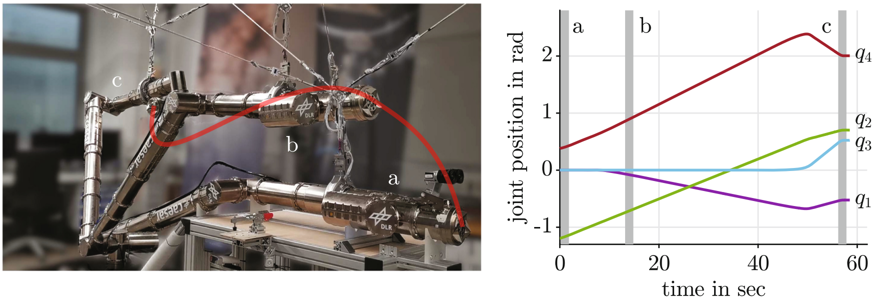

Fig. 5. Multiple exposure image of the moving space robot CAESAR suspended by the MSS. The red line indicates a desired trajectory with (a), (b), and (c) as waypoints along the trajectory. Right: The measured space robot's joint angles with q_1 being the base joint angle.

From experimental data, the *suspension force* ${}_B\boldsymbol{f}_C$ for the shown trajectory is illustrated in Fig. 6 (left) with indicated frames for sequences (a), (b) and (c). The dashed lines show the optimal *suspension forces* ${}_B\boldsymbol{f}_{C,\mathrm{des}}$. The maximum error in the shown force tracking per direction is below 9.5 N which is less than 3.4 % of the requested suspension force. Figure 6 (right) shows the torques of the joints in set A of the CAESAR arm with the sequences (a), (b) and (c) indicated. The dotted lines illustrate simulated joint torques which would be necessary without the mechanical support of MSS in order to compensate gravity. The gray area indicates the torque limitation at ± 80 N m [2] of the space robot. While the joint torques with MSS supporting are below the joint torque limit, the simulated joint torques without MSS support drastically exceed the torque limits by more than factor of 6.

This shows that the trajectory is only possible to be performed with the support of a system such as the MSS. This accounts especially for the torques in joint 2 and 4 (shoulder and elbow), which would need to deliver extremely high

[2] Although joint 5 is located before the coupling mechanism, the MSS does not influence it because the MSS does not apply torque axially on the robotic structure.

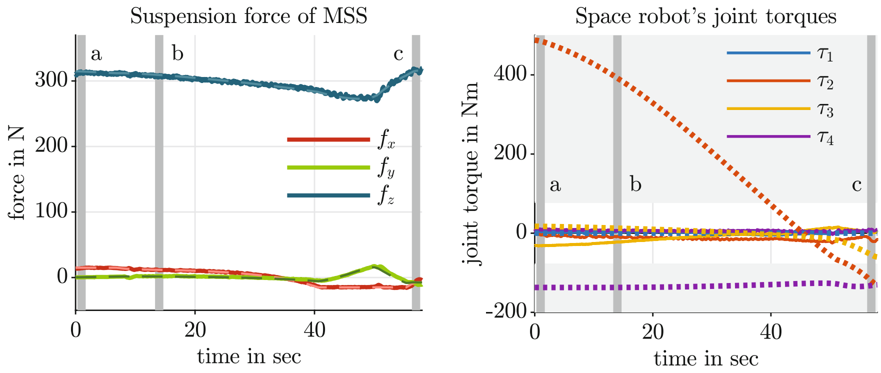

Fig. 6. Left: The *suspension force* ${}_B\boldsymbol{f}_C$ applied by the MSS on the space robot compared with the desired force (dashed line). Right: CAESAR joint torques with (line) and without MSS (dashed line, simulation).

torques up to 480 N m in stretched out configurations such as (a). This experiment highlights the capability of the MSS enabling a space robot to perform three-dimensional movements covering the whole workspace of the space robot.

5 Conclusion and Outlook

This paper presents the MSS, a system that supports a non-gravity-bearing space robot for on-ground tests. It reduces the torque load in the space robot's joints such that the space robot is capable to perform complex, three-dimensional trajectories. This is beyond the capabilities of air bearing systems, which only allow tests in a planar workspace. As a limitation, the MSS does not provide a zero-gravity environment. This would only be possible if every joint or link of the space robot is connected to a suspension unit. However, the presented gravity compensation strategy additionally computes the necessary joint torques for the space robot to reach full gravity compensation. This technology can pave the way for more advanced space robot tests with complex applications, modern algorithms and visual servoing.

As an outlook, other controllers could be explored and compared to the admittance approach in order to improve the tracking performance of the MSS. Inertia and friction could be compensated with an extension of the *Cable Force Calculation* control block (see Fig. 4). This would improve the tracking of the desired gravity compensation force by reducing the impact of hardware flaws. Remote sensor connections instead of cables would simplify the usage. Furthermore, the positioning accuracy of the MSS suffers from static and dynamic effects of the cables such as elongation. Future work aims for evaluating additional sensors such as optical motion tracking for improved position feedback. Additional, improving the cable modeling is planned.

References

1. Aslam, I., Beyer, A., Rostan, M., Kirischian, V., Grunwald, G., Thayer, C., Hiemstra, D., Jimmerson, G., Rettig, T., Schedl, M., Schwarz, S.: How space robotics benefits from the world standard for motion communication. In: 37th Space Symposium, Colorado Springs (2022)
2. Beyer, A., Grunwald, G., Heumos, M., Schedl, M., Bayer, R., Bertleff, W., Brunner, B., Burger, R., Butterfaß, J., Gruber, R., Gumpert, T., Hacker, F., Krämer, E., Maier, M., Moser, S., Reill, J., Roa, M.A., Sedlmayr, H.J., Seitz, N., Albu-Schäffer, A.: CAESAR: space robotics technology for assembly, maintenance, and repair. In: Proceedings of the International Astronautical Congress, Bremen (2018)
3. Brown, D.J.: A novel gravity compensation system for space robots. In: Proceedings of ASCE Specialty Conference on Robotics for Challenging Environments (1994)
4. Carignan, C., Akin, D.: The reaction stabilization of on-orbit robots. IEEE Control Syst. Mag. **10**(1109/37), 887446 (2000). https://doi.org/10.1109/37.887446
5. De Stefano, M., Mishra, H., Giordano, A.M., Lampariello, R., Ott, C.: A relative dynamics formulation for hardware-in-the-loop simulation of on-orbit robotic missions. IEEE Robot. Autom. Lett. (2021). https://doi.org/10.1109/LRA.2021.3064510
6. De Stefano, M., Vijayan, R., Stemmer, A., Elhardt, F., Ott, C.: A gravity compensation strategy for on-ground validation of orbital manipulators. In: IEEE International Conference on Robotics and Automation, pp. 11859–11865. London, UK (2023). https://doi.org/10.1109/ICRA48891.2023.10161480
7. Deremetz, M., Debroise, M., Govindaraj, S., But, A., Nieto, I., De Stefano, M., Mishra, H., Brunner, B., Grunwald, G., Roa, M.A., Reiner, M., Závodník, M., Komarek, M., D'Amico, J., Cavenago, F., Gancet, J., Letier, P., Ilzkovitz, M., Gerdes, L., Zwick, M.: Demonstrator design of a modular multi-arm robot for on-orbit large telescope assembly. In: Symposium on Advanced Space Technologies in Robotics and Automation, Noordwijk, Netherlands (2022)
8. Ding, X., Wang, Y., Wang, Y., Xu, K.: A review of structures, verification, and calibration technologies of space robotic systems for on-orbit servicing. Sci. China Technol. Sci. (2020). https://doi.org/10.1007/s11431-020-1737-4
9. Dungan, L.K., Valle, P.S., Bankieris, D.R., Lieberman, A.P., Redden, L., Shy, C.: Active response gravity offload and method. Patent: US9194977B1 (2015)
10. Flores-Abad, A., Ma, O., Pham, K., Ulrich, S.: A review of space robotics technologies for on-orbit servicing. Prog. Aerosp. Sci. (2014). https://doi.org/10.1016/j.paerosci.2014.03.002
11. Harshe, M., Merlet, J.P., Daney, D., Bennour, S.: A multi-sensors system for human motion measurement: preliminary setup. In: 13th World Congress in Mechanism and Machine Science (2011)
12. Heidel, R., Lemmen, P., Boumann, R., Bruckmann, T.: Design and implementation of a cable-driven robot for automated masonry of building walls. In: Fachtagung VDI Mechatronik, VDI, Darmstadt (2022)
13. Hufnagel, T.: Theoretische und praktische Entwicklung von Regelungskonzepten für redundant angetriebene parallelkinematische Maschinen. Ph.D. thesis, Universität Duisburg Essen (2014)
14. Iturralde, K., Feucht, M., Illner, D., Hu, R., Pan, W., Linner, T., Bock, T., Eskudero, I., Rodriguez, M., Gorrotxategi, J., Izard, J.B., Astudillo, J., Cavalcanti Santos, J., Gouttefarde, M., Fabritius, M., Martin, C., Henninge, T., Nornes, S.M., Jacobsen, Y., Pracucci, A., Cañada, J., Jimenez-Vicaria, J.D., Alonso, R., Elia, L.:

Cable-driven parallel robot for curtain wall module installation. Autom. Constr. (2022). https://doi.org/10.1016/j.autcon.2022.104235

15. Papadopoulos, E., Paraskevas, I., Flessa, T., Nanos, K., Rekleitis, Y., Kontolatis, I.: The NTUA space robot simulator: design and results. In: 10th ESA Workshop on Advanced Space Technologies for Robotics and Automation (2008)
16. Papadopoulos, E., Aghili, F., Ma, O., Lampariello, R.: Robotic manipulation and capture in space: a survey. Front. Robot. AI (2021). https://doi.org/10.3389/frobt.2021.686723
17. Pedemonte, N., Rasheed, T., Marquez-Gamez, D., Long, P., Hocquard, É., Babin, F., Fouché, C., Caverot, G., Girin, A., Caro, S.: FASTKIT: a mobile cable-driven parallel robot for logistics. In: Advances in Robotics Research, Springer Tracts in Advanced Robotics, pp. 141–163. Springer International Publishing, Cham (2020). https://doi.org/10.1007/978-3-030-22327-4_8
18. Pott, A.: Cable-Driven Parallel Robots: Theory and Application. Springer Tracts in Advanced Robotics. Springer, Berlin (2018). https://doi.org/10.1007/978-3-319-76138-1
19. Pott, A., Bruckmann, T., Mikelsons, L.: Closed-form force distribution for parallel wire robots. In: Kecskeméthy, A., Müller, A. (eds.) Computational Kinematics, pp. 25–34. Springer, Berlin (2009). https://doi.org/10.1007/978-3-642-01947-0_4
20. Reichert, C., Bruckmann, T.: Unified contact force control approach for cable-driven parallel robots using an impedance/admittance control strategy. In: Proceedings of the 14th IFToMM World Congress (2015)
21. Sawada, H., Ui, K., Mori, M., Yamamoto, H., Hayashi, R., Matunaga, S., Ohkami, Y.: Micro-gravity experiment of a space robotic arm using parabolic flight. Adv. Robot. (2004). https://doi.org/10.1163/156855304322972431
22. Schwartz, J.L., Peck, M.A., Hall, C.D.: Historical review of air-bearing spacecraft simulators. J. Guid. Control. Dyn. **10**(2514/2), 5085 (2003). https://doi.org/10.2514/2.5085
23. Wu, Y., Cheng, H.H., Fingrut, A., Crolla, K., Yam, Y., Lau, D.: CU-brick cable-driven robot for automated construction of complex brick structures: from simulation to hardware realisation. In: 2018 IEEE International Conference on Simulation, Modeling, and Programming for Autonomous Robots (SIMPAR). IEEE, Brisbane, QLD (2018). https://doi.org/10.1109/SIMPAR.2018.8376287
24. Yao, H., Ren, W., Ma, O., Chen, T., Zhao, Z.: Understanding the true dynamics of space manipulators from air-bearing based ground testing. J. Guid. Control. Dyn. **10**(2514/1), g003501 (2018). https://doi.org/10.2514/1.G003501
25. Zarebidoki, M., Dhupia, J.S., Xu, W.: A review of cable-driven parallel robots: typical configurations, analysis techniques, and control methods. IEEE Robot. Autom. Mag. (2022). https://doi.org/10.1109/MRA.2021.3138387